Detection and Identification of High Impedance Faults in Single Wire Earth Return Distribution Networks

M. Kavi, Y. Mishra, and D.M. Vilathgamuwa

School of Electrical and Computer Engineering, Faculty of Science and Engineering, Queensland University of Technology, Brisbane, Australia

Abstract **- Single Wire Earth Return (SWER) system is an inexpensive method for extending power to remote areas in scantly populated countries such as Australia. SWER network introduces several challenges to the conventional methods for protection relays. This paper focuses on the protection aspect of the SWER network and investigates the effectiveness of the existing conventional protection mechanism in detecting and suppressing common fault conditions including High Impedance faults (HIFs). While the existing SWER distribution network protection system can detect HIFs, it may be often taken as a normal step load increase due to the low fault current levels. The persistence of the HIFs compromises safety of people within the vicinity of the fault and also increase risk of fire, therefore, a new protection strategy for the detection and identification of HIFs to mitigate the risks is necessary. This paper presents a new algorithm based on mathematical morphology, called the Decomposed Open-Close Alternating Sequence, (DOCAS) for the detection and identification of any power system disturbances in SWER systems. The effectiveness of the proposed method in the detection and identification of the High Impedance Fault and differentiate with other conditions such as Single line-to-ground (SLG) fault and step load increase is demonstrated. The simulation results show that the HIFs can be clearly distinguished from the other conditions by analysing the transients generated by the HIFs.**

Indexed Terms**- Power system protection, Single Wire Earth Return Network, High Impedance faults mathematical morphology**

I. INTRODUCTION

The Single Wire Earth Return (SWER) system is a cost effective method of extending the electricity distribution to the rural and dispersed communities who are far off from the electricity supply grid. It uses a single active conductor and the earth as return path for the current. The conductor is connected to the earth by buried earth electrodes at the source and load to provide the return path. A schematic representation of a typical SWER network arrangement is shown in Fig.1. The starting point of the SWER network is the Isolating Transform.

978-1-5090-1405-7/16/$31.00 ©2016 IEEE

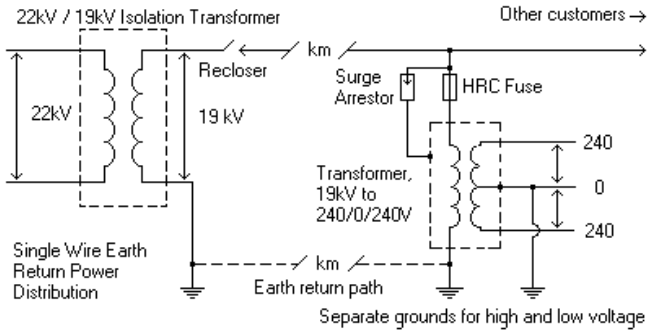

Fig.1: Single Wire Earth Return (SWER) distribution network arrangement, [1]

The two primary winding terminals of the isolating transformers connect directly to two phases of the substramission line which is normally at 22kV.

The SWER distribution system voltage is normally at 19.1kV or 12.7kV taken between the active conductor and the earth on the secondary side of the isolation transformer. Noticeably there is no earth connection on the primary side of the isolation transformer; hence there is no earth connection between the SWER network and three-phase feeder transmission network. The implication of such arrangement is that, in the event of an earth fault, the fault current (primarily zero sequence current) will not flow back to the feeder substation. Thus, the SWER fault will not be cleared by the upstream feeder protection system. The SWER distribution network must have its own protection system to suppress any dangerous operating conditions due to faults and other abnormalities, [1-4]. The three main conditions considered in this paper that would cause an increase in the current magnitude in the SWER distribution network includes, a Single Line-to-Ground (SLG) Fault, a sudden (step) increase in the consumer load and High Impedance Fault (HIF). The SLG is a permanent fault that can result in a high fault current, and if allowed to persist will cause damage to the network devices. The step load increase can be considered as normal operation. The transients generated by the load switching and the steady state load current are usually below the thermal limit of the conductor and the threshold setting of the Automatic Circuit Recloser (ACR). Occurrence of HIFs can either be transient, when tree branches or limbs come into momentary contact with the conductor or can be permanent

when a tree branches or limbs are in permanent contact with the conductor. Moreover, permanent cases of also HIFs occur when the fallen conductor either broken or otherwise comes into contact with ground, grass, gravel, or any high impedance surfaces. Due to the high impedance of the contact surfaces, the HIFs, either transient or permanent generate low fault current which is below the threshold setting of the ACR, thus making it difficult for the protection device to operate and isolate these faults. Furthermore, the slight increase in the level of fault current due to HIFs cannot be easily distinguished from the increase in the current due to load increase thus allowing the HIFs to persist.

The Automatic Circuit Recloser (ACR) is the critical element in the deployment of overcurrent protection in the SWER distribution network. The ACR combines a circuit breaker (CB) with digital relay functionality to discriminate between normal and abnormal normal conditions. The ACR in conjunction with current transformer (CT) monitors the current level on the SWER distribution network, and if abnormal current, higher than the threshold setting, which is normally at more than twice the full load current is detected, the CB is caused to trip to isolate the fault. Furthermore, the ACR also incorporates automatic reclosing functionality where the CB automatically recloses to restore power if the abnormal condition is a simple transient caused by momentary condition such as a tree branch coming in contact with the conductor, [5]. However, if the fault is of permanent nature and/or with low fault level (such as HIFs), it is hazardous as the fallen conductor is energised by the closing action of the ACR. Arcing will occur thus increasing the risk of fire and safety of people within the vicinity. Furthermore, the ACR has no mechanism to detect and differentiate a HIF from a normal load increase. Thus the fault persists and the risks remain as long as the conductor remains energised. Therefore, the existing SWER protection cannot provide effective protection against HIFs.

Australia utilises SWER technology for large distance rural networks. Recently, the Royal Commission Enquiry on Victorian bush fire that killed many people in 2009 has identified the SWER distribution network as the major contributor to the risk of bushfire [6]. In this paper, preliminary results of the proposed algorithm for the detection and identification of power system disturbances performed on an example SWER network for the three major conditions as mentioned are presented. In section II, the characteristic of the algorithm is presented followed by the simulated results in Section III.

II. PROPOSED ALGORITHM FOR THE FAULT DETECTION AND IDENTIFICATION

A new algorithm based on Mathematical Morphology (MM) called, Decomposed Open-Closed Alternating Sequence (DOCAS) is proposed by the authors for the detection and identification of power system disturbances including HIFs in distribution networks including SWER networks. MM is a nonlinear image and signal processing technique that is based on set theory and lattice algebra, [7-9]. The version of MM used in signal processing is called "Gray-scale MM", where the signal is considered as one dimensional image represented by its graph on the Cartesian Coordinate or Euclidian Space. The geometrical features of the signal under consideration is decomposed by a filtering or probing signal called, a "Structuring Element, (SE)" to extract the hidden characteristics in complete time domain for fault detection and identification. The two primitive MM transforms from which every other transform is derived from are dilation and erosion [5]. Suppose $f(n)$ is the fault signal in the domain $\mathcal{D}_f(n) = \{n_o, n_1, n_2, \ldots n_n\}$, and $g(m)$ is the SE in the domain $\mathcal{D}_g(m) = \{m_o, m_1, m_2, \ldots m_m\}$ where n and m are integers such that $n > m$. The pointwise dilation and erosion of $f(n)$ by $g(m)$ is given by (1) and (2) respectively.

$$f_d(n) = (f \oplus g)(n) = \max\{f(n-m) + g(m)\}, \quad 0 \le (n-m) \le n, m \ge 0. \qquad (1)$$

$$f_e(n) = (f \Theta g)(n) = \min\{f(n+m) - g(m)\}, \quad 0 \le (n+m) \le n, m \ge 0. \qquad (2)$$

where $f_d(n)$ and $f_e(n)$ are the dilated and eroded versions of the fault signal $f(n)$ respectively by $g(m)$. The physical effect is that each point on the signal $f(n)$ increases in size by dilation whereas erosion decreases the size. The two derivatives of the primitive transforms MM used in the proposed algorithm are the Opening and Closing transforms as given in (3) and (4) respectively.

$$f_o(n) = (f \circ g)(n) = ((f \Theta g) \oplus g)(n) \qquad (3)$$

$$f_c(n) = (f \bullet g)(n) = ((f \oplus g) \Theta g)(n) \qquad (4)$$

The Opening and Closing transforms recover the features of the signal due to dilation and erosion of the signal respectively. The Opening transform reduces the small positive region while the Closing transform reduces the small negative region within the signal. These characteristics are the foundation for feature extraction for fault detection and identification in the proposed algorithm. MM based algorithms have been proposed in the past for the detection and identification of various power system disturbances. An evaluation of different filter operations such as, dilation, erosion, opening and closing, from which a conclusion was drawn to have an adaptive generalized MM filter for the detection of power system disturbances with a flat structuring element, was provided by [10]. References [11, 12] proposed MM based analysers with flat SE, for the detection of various power system disturbances. Another proposal for an adaptive MM based filter combination of opening-closing and closing-opening operations based on Minimum Mean Square Error with appropriate selection of structuring elements suitable for each condition for the monitoring of the power quality was provided by [13]. Combination of different MM functions have been proposed by [14] for the detection of different

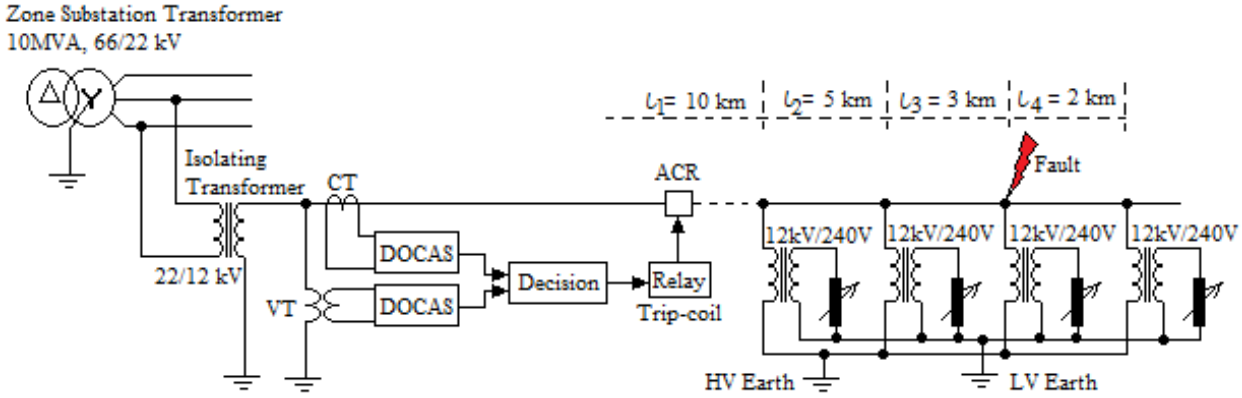

Fig 2: Example SWER distribution network used in the simulations

power system disturbances. The most notable of the proposed MM algorithms is for the detection of HIFs, [9].

All the proposed MM algorithms use flat SEs with different sizes, and while they have been tested by simulation with some degree of success for the different purpose they were designed for, the proposed algorithms are for specific power system condition, and may not be effective in another condition. Moreover, the use of flat SE may result in unrealistic result, [8].

The proposed algorithm utilises the fundamental MM transforms in a strategic manner to form a cascaded multistage morphological fault detector using a weighted SE to give robustness**.** Two stages of decomposed Morphological Median Filters are used for the fault detection and two layers of four stage Alternating Sequential (Open-Close and Close-Open) filters are used for feature extraction. The effectiveness of the MM algorithm depends on the design and careful selection of the Structuring Element (filtering signal). The geometrical shape of the SE used in the proposed algorithm is defined by (5).

$$SE = \cos(2\pi fm\Delta T) \quad (5)$$

where m is the number of points on the SE, such that $1 \leq n \leq m$, thus resulting in the SE having an odd length of $(2n + 1)$. The other elements are, f which is the fundamental frequency and sampling interval, ΔT. Based on the 50Hz fundamental frequency and a sampling of 3200 Hz, the sampling interval is 312.5 µs. The generalised SE given in (5) is decomposed into two linearly SEs and used in the different stages of the proposed algorithm. The features of the algorithm include detection of the fault condition within a fixed data window of a quarter cycle of the fundamental period. A further two data windows may be required to identify the fault after detection. Based on the sampling interval used in the design, a data window size is only 16 samples, thus resulting in fast detection of the fault.

III. SIMULATIONS AND DISCUSSIONS

The proposed algorithm will be located at the SWER substation to continuously monitor the SWER line current and voltage levels taken from the secondary of the CT and VT respectively. The SWER system used in the simulation is an example system shown in Fig.2. The example SWER distribution network was modelled in MATLAB/Simulink with parameters as specified. The SWER network has a total length of 20 km with per unit parameter values of R = 1.828 Ω and L = 0.7404×10^{-3} H at 50 kHz. The Isolating transformer is 1 MVA, 22kV/12.7kV. The average consumer load is 200kW fed through consumer transformers of 250 kVA and 12.7kV/240V ratings. Earthing resistance of 1Ω and 5Ω were used for the LV and HV earths respectively.

The three main conditions simulated in this paper are SLG, HIF and Load Increase at the midpoint in the SWER network. The simulation results are based on the line parameters and load condition used in this example SWER distribution network. In the simulations, the SWER line current is taken as input signal for fault detection and identification. The SWER line voltage could also be considered as the input, or both current and voltage can be taken as input signals as the algorithm allows for multiple input signals.

A. Single Line-to-Ground Fault

A SLG fault occurs at 0.02s at the fault point on the SWER line. The fault current waveform is shown in Fig.3.The current waveform has been normalized between +1 and -1 to cater for different fault current levels. The corresponding DOCAS algorithm output to the SLG is shown in Fig.4. The first spike on Fig.4 at 0.02s is equal to 1 as the slope on the fault current waveform is very steep due to the occurrence of the fault. The subsequence windows give the steady-state fault current. Since two windows (half cycle) are used for detection and identification, the second and subsequent spikes represent the steady-state fault current as there is no DC-offset in this case. Thus the per unit fault level is, '*steady state fault level' - 'prefault level'*. The prefault level from Fig.4 is 0.05 and the steady state fault level is 0.99 giving a per unit fault current increase of 0.94. For this example, SWER network, the fault current due to SLG increases by

1880%. This will trip the ACR and to isolate the fault as the normal threshold setting of the ACR is normally not less than 200% of the full load current, [5]. The fault level will vary depending on the fault location. However, the fault current due to a single line-to-ground fault occurring at any point in the SWER network will still be large enough to trip the ACR and keep it de-energized.

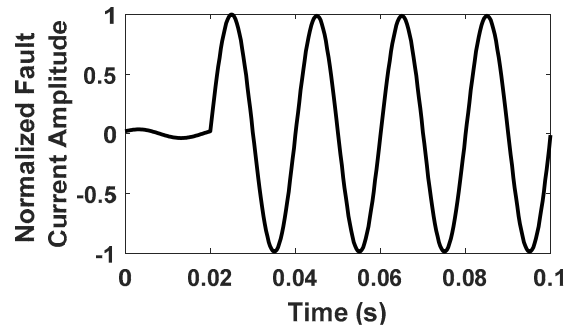

Fig. 3: Single Line-to-ground fault current waveform for fault at 0.02s

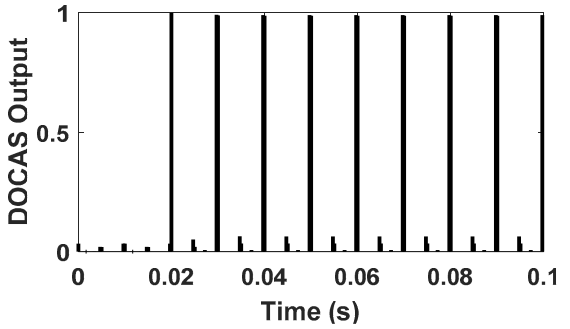

Fig. 4: Morphological Fault Detector (DOCAS) Output for SLG fault current signal

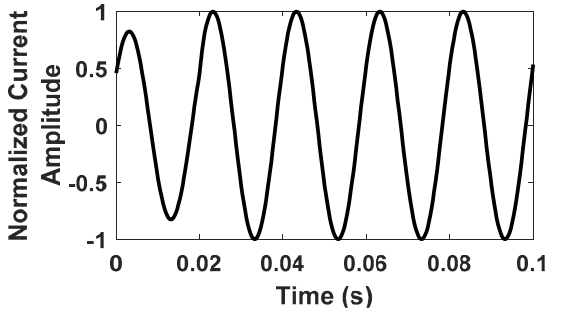

Fig. 5: Load Current waveform for step load increase at 0.02s

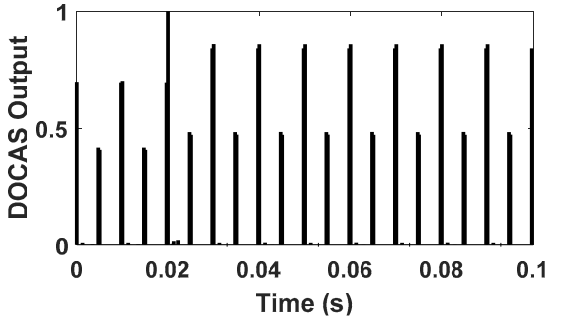

Fig. 6: Morphological Fault Detector (DOCAS) Output for step load increase current signal

B. Step Load Increase

A step load increase of 200W by the second consumer occurs at 0.02s. The load current increase and the associated DOCAS output are shown in Fig.5 and Fig.6 respectively. The per unit prefault current is 0.7 and steady state current after the load increase is 0.855 from Fig.6. This gives a per unit load current increase of 0.155. Thus, the load current only increases by 22.14%. This is way below the threshold setting of the ACR, thus it will not be activated, and the SWER network will continue operation.

C. High Impedance Fault

A recommendation by the IEEE Power Systems Relaying Committee, (PSRC) Working Group is that HIF fault studies be conducted at voltage levels of 15kV or below, [9], [15]. The SWER distribution system voltage operates at either 12.7kV or 19.1kV levels. Simulations were conducted on both voltage levels, and it was observed that results were comparable; hence, observations and conclusions apply to both voltage levels. Several different arc models have been proposed in the past by various researchers based on staged tests and laboratory based tests. These models, while may be structurally different, must encapsulate following fundamental features of the HIFs; arcing, unsymmetrical and intermittency in the fault current, harmonic and high frequency content of the fault current, nonlinearity and the random nature of the fault resistance, [16-18]. A simple HIF model, yet captures the fundamental characteristics is the Emmanuel arc model of Fig.7. This is the HIF arc model used in this simulation study.

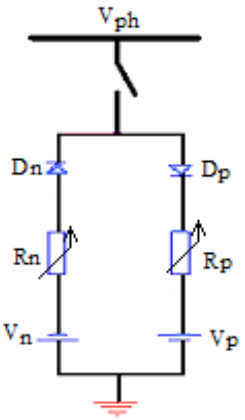

Fig.7: Emmanuel HIF arc model, [18]

The HIF was simulated by connecting the HIF arc model between the SWER line and ground at the point of fault on Fig.2.The SWER line voltage is represented by V_{ph}. The DC voltage sources, V_p and V_n connected in series with respective diodes have unequal magnitude and vary randomly to model the unsymmetrical positive and negative half cycle of the fault current. The resistance R_p and R_n represent the arc resistance, and vary randomly to model arcing phenomena of HIF. From past researches, it was shown that the HIF current range is 10A-50A [19-20]. Moreover, the HIF current magnitude is subjected to the high impedance contact surface

and the arc radius. Considering the SWER distribution network load capacity, it is reasonable to assume that the load current would be of low magnitude, and hence will also impact on the HIF current magnitude. Thus, the parameters on the HIF arc model have been scaled to permit a maximum HIF current of 10A with a variance of ±10%. The following parameter values have been used in this simulation, V_p = 1kV, V_n = 0.5kV, R_p = 1kΩ and R_n = 1kΩ all with variance of ±10%. A case of permanent HIF was simulated at the fault point on the SWER line occurring at 0.02s. Fig.8 shows the HIF current to ground. This waveform has unsymmetrical positive and negative half cycles. Depending on the nature of the contact surface and arc resistance, the waveform will be shoulder shaped representing the zero-crossing and the momentary extinguishing and reigniting of the arc. This is not the fault current detected by the ACR. The HIF induced fault current on the SWER line is given in Fig.9, and this is the current seen by the ACR. The SWER line fault current of Fig.9 is reduced by the CT ratio of 500 and normalized between +1 and -1 to cater for different fault current levels. The associated DOCAS output of the HIF SWER line current is shown in Fig.10. The per unit prefault current is 0.15 and the steady state fault current after fault initiation at 0.02s is 0.29 giving a per unit fault current increase of 0.110. The fault current increases by 93.33%. This is well below the 300% threshold setting of the ACR; hence the conductor will remain energised. Moreover, the magnitude increase in the fault current due to the HIF does not differentiate it from the magnitude increase in the load current due to a load increase as both values are below the threshold setting of the ACR for overcurrent protection.

The HIFs have several distinguishing characteristics, [19, 21-22]; however, a specialized algorithm using a reliable and efficient signal processing technique such as the DOCAS algorithm based on Mathematical Morphology is required for the detection and identification of HIFs. One of the identifying characteristics of the HIFs is the transients generated by HIFs. The DOCAS algorithm decomposes the fault signal (current/voltage) input to extract information for fault identification based on the transient caused by the HIFs. To differentiate between a step load increase and a HIF, consider the DOCAS output of Fig.6, and Fig.9 and Fig.10. In Fig.10 there are appearances of additional spikes. These are clearly visible in the expanded DOCAS output of Fig.9. These spikes are generated by the HIF transients. Fig.6 does not have these spikes. The spikes due to the HIF repeat after every consecutive second data window after the fault inception. These spikes will continue to appear as longs as the fault exist. Moreover, the number of spikes appearing depends on the size of the arc impedance which depends on the arc radius. As it can be observed in Fig.11, there are two spikes in the 0.025s to 0.03s data window where as there is only one spike in the 0.035s to 0.04s data window. This is because in the positive half cycle the fault resistance is of different value than in the negative half. Moreover, the spikes appear towards the end of the 5ms data window, thus the spikes reappear after every 10ms. This is the distinguishing feature of the HIF from the load increase.

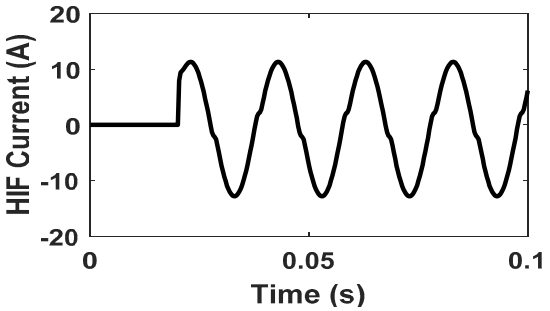

Fig. 8: High Impedance Fault current for fault at 0.02s

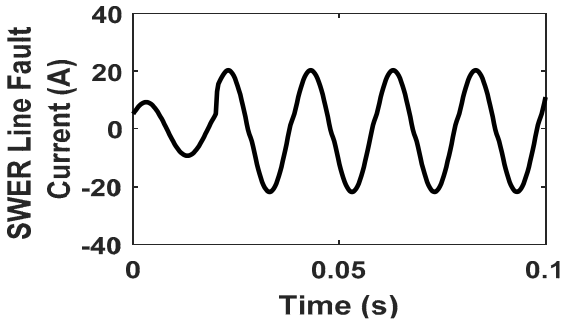

Fig. 9: High Impedance Fault SWER Line fault current for fault at 0.02s

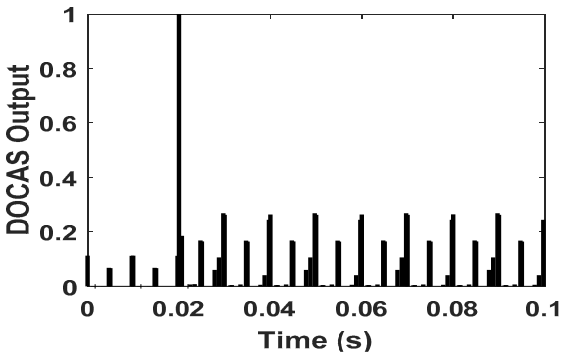

Fig. 10: Morphological Fault Detector (DOCAS) output for HIF SWER Line fault current

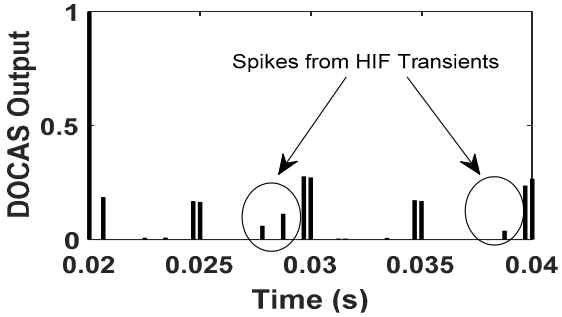

Fig. 11: DOCAS Output of HIF SWER Line fault showing spikes generated due to HIF transients

The tripping action can be either automatic, where a trip signal is initiated to trip the CB or an alarm can be initiated for manual tripping. Simulation of other conditions such as arc welding, capacitor switching and induction motor load switching will need to be considered to further differentiate

these as well from HIFs before a decision logic is developed for initiating the breaker trip sequence.

IV. CONCLUSIONS

Power system disturbances and faults resulting in suboptimal power system operation or complete system failure cannot be completely eliminated. However, with effective protection strategy utilizing specialized fault detection algorithms, the impact of such difficult faults as High Impedance Faults can be mitigated. Although impact of HIFs may not be of immediate concern to power system equipment and devices, its continuous presence is a fire hazard and a safety risk for people within the vicinity of the fault. As it has been shown, the existing protection mechanism within the power system networks, more so in the SWER distribution network has not means of detecting HIFs. Preliminary simulated results of the proposed DOCAS algorithm show that it is possible to detect and identify HIFs, and other power system events. Such algorithm can operate in tandem to complement the existing protection system to effectively detect and isolate any fault conditions. Once a fault condition such as HIF is detected, an alarm or alert can be issued for manual isolation. With further functional characteristics as fault location estimation, the appropriate breaker can be automatically tripped.

REFERENCES

[1] Wikipedia, "Single wire earth return" https://en.wikipedia.org/wiki/Single-wire_earth_return, 2016

[2] H. Nasser, J.E. Mayer, and P. J. Wolfs. "Rural Single Wire Earth Return distribution networks–Associated problems and cost-effective solutions." *International Journal of Electrical Power & Energy Systems*, Vol. 33, no. 2, pp: 159-170, Feb 2011

[3] M. A. Kashem, and G. Ledwich. "Impact of distributed generation on protection of single wire earth return lines." *Electric Power Systems Research*, Vol. 62, no. 1, pp: 67-80, may 2002.

[4] J. Mayer, N. Hossein-Zadeh, and P. Wolfs. "Investigation of voltage quality and distribution capacity issues on long rural three phase distribution lines supplying SWER systems." *AUPEC 2005 Proceedings* 2, pp : 392-395, Sep 2005.

[5] G.F Peirson, A. H. Pollard, and N. Care. "Automatic circuit reclosers." *Proceedings of the IEE-Part A: Power Engineering* Vol. 102, no. 6, pp: 749-764, Dec 1955

[6] Victorian Government Response to The Victorian Bushfires Royal Commission Recommendations 27 and 32, "*Power Line Bushfire Safety Taskforce Report*", *Dec, 2011*

[7] Q. H. Wu, Z. Lu, and T. Ji, " Protective relaying of power systems using mathematical morphology". *Springer Science and Business Media.,* 2009.

[8] F.Y. Shih, " Image processing and mathematical morphology: fundamentals and applications" *CRC press.,* 2009

[9] S. Gautam, and S. M. Brahma, "Detection of high impedance fault in power distribution systems using mathematical morphology." *Power Systems, IEEE Transactions on* 28, no. 2 ,2013

[10] Y. Tingfang, L. Pei., Z. Xiangjun, and K. Li, "Application of adaptive generalized morphological filter in disturbance identification for power system signatures," in *International Conference on Power System Technology, 2006. PowerCon 2006., Oct. 2006* pp. 1-7

[11] G. Li, M. Zhou, Y. Luo, and Y. Ni, "Power quality disturbance detection based on mathematical morphology and fractal technique". In *Transmission and Distribution Conference and Exhibition: Asia and Pacific, 2005 IEEE/PES*, 2005, pp. 1-6.

[12] Z. Lu, D. R. Turner, Q. H. Wu, J. Fitch, and S. Mann, "Morphological transform for detection of power quality disturbances". In *International Conference Power System Technology, 2004. PowerCon 2004.* Vol. 2, Nov. 2004, pp. 1664-1649 .

[13] Sen, Ouyang, and Ren Zhen. "Application of improved mathematical morphology method in the power quality monitoring." In *Power System Technology, 2006. PowerCon 2006. International Conference on*, pp. 1-6. IEEE, 2006.

[14] S. Gautam, and S.M. Brahma. "Guidelines for selection of an optimal structuring element for mathematical morphology based tools to detect power system disturbances." *Power and Energy Society General Meeting, 2012 IEEE*. IEEE, 2012.

[15] J. Majid, R. Singh, and S. K. Sharma. "High Impedance Fault Detection in Electrical Power Feeder by Wavelet and GNN." In *International Journal of Engineering and Applied Sciences,Vol.2,no.2, Mar 2015*

[16] A.R. Sedighi, and M-R. Haghifam. "Simulation of high impedance ground fault In electrical power distribution systems." *Power System Technology (POWERCON), 2010 International Conference on*. IEEE, 2010.

[17] F. Setayesh, S. M. H. Hosseini, and S. Mogharabian. "High Impedance Faults Modeling in Electrical Power Distribution Networks."

[18] V. Torres, J.L. Guardado, H.F. Ruiz, and S. Maximov, S. (2014). Modeling and detection of high impedance faults. *International Journal of Electrical Power and Energy Systems*, *no. 61, pp: 163-172, 2014*

[19] F.B. Costa, B. A. Souza, N. S. D. Brito, J. A. C. B. Silva, and W. C. Santos. "Real-Time Detection of Transients Induced by High-Impedance Faults Based on the Boundary Wavelet Transform." *Industry Applications, IEEE Transactions on vol. 51, no. 6, pp: 5312-5323, 2015*

[20] M.T Yang, J.C. Gu, J.L Guan, and C.Y. Cheng, C. Y, "Evaluation of algorithms for high impedance faults identification based on staged fault tests". In *Power Engineering Society General Meeting, 2006. IEEE pp: 8-pp, IEEE.*

[21] A.H. Eldin, E.Abdallah and N.Mohamed, "Detection of high impedance faults in medium voltage distribution networks using discrete wavlet transform. "In *Electricity Distribution (CIRED 2013), 222nd International Conference and Exhibition on, pp:1-4, IET 2014*

[22] N. Zamanan, and J. Sykulski, "The evolution of high impedance fault modeling". In *Harmonics and Quality of Power (ICHQP), 2014 IEEE 16th International Conference on*, *pp. 77-81, IEEE May, 2014*